Development of Tools for the Design of Selectin Antagonists

Hartmuth C. Kolb* and Beat Ernst

Dedicated to Professor Hans Paulsen on the occasion of his 75th birthday

Abstract: A molecular modeling tool for the rational design of E-selectin antagonists based on the lead structure sialyl Lewis^x has been developed. The binding affinity to the receptor is considerably influenced by the entropy and consequently by the antagonist's ability to place its pharmacophores in an optimal spatial arrangement, i.e., by its preorganization for binding. The computational model assesses the preorganization of a potential selectin antagonist with the aid of Monte Carlo (jumping between wells)/stochastic dynamics [MC(JBW)/SD] simulations. The model has been validated by correlating preorganization and bioactivity of several selectin antagonists. The results suggest that only preorganized compounds are likely to bind to E-selectin.

Keywords
carbohydrates · molecular modeling · preorganization · sialyl Lewis^x · selectins

Introduction

Carbohydrate/lectin interactions play an important role in cell recognition processes.[1] Interactions of sialyl Lewis^x bearing glycopeptides and -lipids with a family of C-type lectins, the so called selectins, are responsible for the "rolling" event, which is the first step in the multistage process of leukocyte recruitment to sites of injury or inflammation.[2] This recruitment process plays a crucial role in a number of diseases and pathological situations, for example, inflammation, reperfusion injury, rheumatoid arthritis, metastasis, and angiogenesis.

Currently, substantial research efforts are being concentrated on the development of carbohydrate-derived drugs that interfere with the rolling stage of the inflammatory response by blocking the selectin binding site.[2] The design of sialyl Lewis^x mimics requires a thorough understanding of the structure/activity relationship as well as the bioactive conformation. The latter describes how the carbohydrate ligand presents itself to the binding site (Figure 1).

The results from structure/activity studies undertaken by us and other groups[3] may be summarized as follows: The presence of all three OH groups of fucose, the 4- and 6-OH group of galactose, and the COOH group (negatively charged) of neuraminic acid is essential for binding to E-selectin. In contrast, the 2-OH group of galactose and the side chain of neuraminic acid are not required.

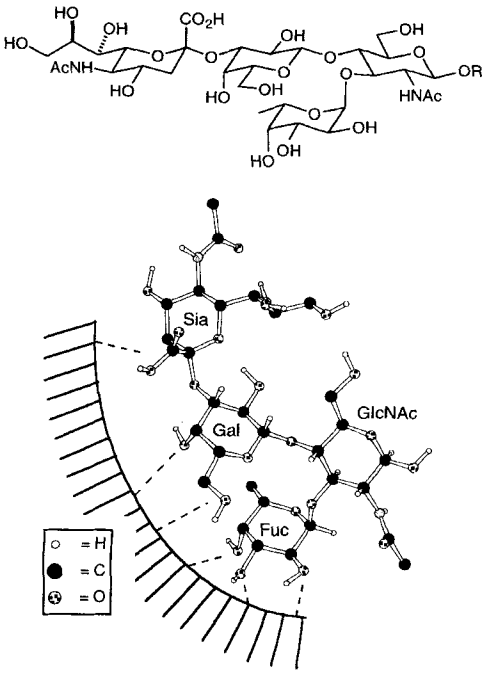

Figure 1. Top: sialyl Lewis^x. Bottom: Bioactive conformation of sialyl Lewis^x and schematic representation of its binding to E-selectin.

The bioactive conformation, recently determined by transfer-NOE NMR studies[4] on the sialyl Lewis^x/E-selectin complex, is shown in Figure 1. The most characteristic feature is the stacking of the galactose and fucose units with the GlcNAc portion acting as a spacer. The neuraminic acid/galactose linkage, which has been shown to be the most flexible interglycosidic linkage, adopts the conformation shown in Figure 1 (bot-

[*] H. C. Kolb, B. Ernst
Novartis Pharma Ltd., Rosental R-1060.3.34, CH-4002 Basel (Switzerland)
Fax: Int. code +(61)697-8975
e-mail: beat.ernst@chbs.mhs.ciba.com

  0947-6539/97/0310-1571 $ 17.50+.50/0

tom).[4] This is in contrast to NMR[5] and molecular modeling[5a, 6] results on the free sugar, which suggest the presence of several conformations in aqueous solution.

The free binding energy between the carbohydrate and the selectin is a function of the binding enthalpy and the binding entropy. The former is directly dependent on the number and the strength of carbohydrate/lectin contacts, while the latter is influenced by the flexibility of the carbohydrate ligand and its propensitiy to adopt the bioactive conformation. The flat nature of the receptor's binding site[7] is consistent with the observation that not all of the ligand's functional groups are involved in binding, suggesting that the ligand/receptor interactions are distributed over a relatively wide area. Consequently, the spatial orientation of the functional groups involved in binding considerably influences the free interaction energy by way of the entropy. The binding affinity may, therefore, be enhanced by designing ligands favoring the bioactive conformation, that is, preorganized for binding.

We now describe a molecular modeling tool for assessing the flexibility and the preorganization of sialyl Lewis^x mimics for binding to E-selectin. This method is based on simulation techniques recently developed by Still and co-workers.[8, 9] Thus, the potential energy surface of the mimic is probed by a Monte Carlo (jumping between wells)/stochastic dynamics [MC(JBW)/SD] simulation,[9] which generates a Boltzman weighted ensemble of states by jumping between different energy wells and performing stochastic dynamics simulations within each well. These energy wells are conformers that have been identified in a preceding conformational search in torsional space by using the systematic unbounded multiple minimum (SUMM) method.[8]

Computational Methods

The force field and the solvent model: The basis for the calculations is the Amber* force field as implemented in MacroModel 5.0.[10] It has recently been optimized for carbohydrates in an united atom approach by Still et al.[11] The rotational profiles of carbohydrate structural elements are similar both in the united and all-atom versions of the force field. We consistently employ an all-atom approach for our simulations. In addition, we have improved the parameters for α-alkoxycarboxylic acids, an important structural element in sialyl Lewis^x and its mimics. Recent studies by Tvaroska et al.[6] and Rockwell et al.[13] have shown the solvent to have a large influence on the conformational equilibria of interglycosidic linkages and cyclohexanediol derivatives, respectively. Consequently, the force field calculations of sialyl Lewis^x and its mimics were performed using Still's "generalized born/solvent accessible surface area" (GB/SA) continuum model for water.[14] Still and co-workers[11] have recently used this GB/SA solvent model in conjunction with the MC(JBW)/SD technique and the united atom Amber* force field for the calculation of anomeric free energies of pyranoses, and a good agreement with observed values was obtained.

The generation of a Boltzman weighted ensemble of states: Conventional molecular dynamics simulations suffer from low interconversion rates between states separated by large energy barriers. The MC(JBW)/SD procedure[9] circumvents this problem by forcing the molecule to jump between the energy wells. Metropolis sampling is used for each jump in order to generate an ensemble which approximates the correct Boltzman distribution. The input for the MC(JBW)/SD simulation is a set of 100 low-energy conformations (up to 20 kJ mol^{-1} above the global minimum) obtained in a systematic conformational search using the SUMM procedure.[8] The MC(JBW)/SD simulations were performed between 2 and 10 ns at 300 K in GB/SA water using the Amber* force field, and structures were sampled every 1 ps (2 ps for the 10 ns simulations). The convergence of each simulation was checked by a) calculating the relative time in each energy well, b) determining the frequency of successful jumps, and c) following ensemble averages, such as the relative population of certain areas in conformational space, as a function of time. These tests showed that all the calculations were converged within 1 to 2 ns. The acceptance rate of the MC(JBW) part of the 10 ns simulation was 32% for sialyl Lewis^x and interconversion between different conformations occurred once every 23.5 ps on average.

Data analysis and data reduction: We use a two-dimensional internal coordinate system to define the spatial arrangement of the relevant pharmacophores, namely, that of the COOH group relative to the fucose moiety. One coordinate, the Fuc(C4)-Fuc(C1)-Fuc(O1)-Acid(Cα) angle (Figure 2a), describes the conformation of the Lewis^x core and is independent of the actual nature of the core. The other coordinate, the angle Fuc(C1)-Fuc(O1)-Acid(Cα)-Acid(*C*=O) (Figure 2b), defines the orientation of the COOH group relative to the core. The data from both the initial conformational analysis as well as the subsequent MC(JBW)/SD simulation are analyzed by means of this internal coordinate system.

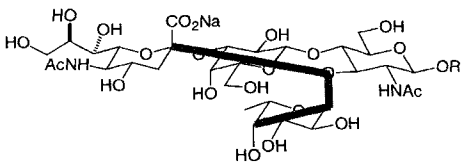

(a) Core Conformation

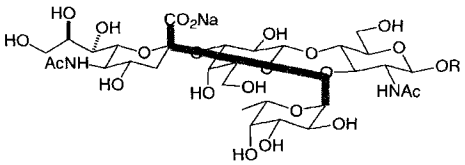

(b) Acid Orientation

Figure 2. Internal coordinates.

Each conformer, found in the initial conformational analysis (SUMM), is shown as a point in an internal coordinate plot, and its energy is color-coded (Figure 3a); bright colors represent low energy and dark colors high energy. The several thousand structures obtained in the MC(JBW)/SD simulations are used to evaluate the probability for being at any point of the two-dimensional torsional space at a resolution of 3° by 3°. These probability data are presented in the two-dimensional internal coordinate system, by means of a color code (Figure 4a); bright colors represent high probability and dark colors low probability.

Results and Discussion

Validation of the method by correlating calculations and experimental data on the bioactive conformation of sialyl Lewis^x: According to the conformational SUMM search,[8] four clusters (A–D) in conformational space are within 20 kJ mol^{-1} of the global energy minimum in sialyl Lewis^x (Figure 3a), suggesting a moderate flexibility of the carbohydrate[5, 6] and raising the question as to which of these clusters is responsible for bioactivity. The three-dimensional representation of the global minimum conformation, belonging to cluster "A", is shown in Figure 3b. The interglycosidic torsional angles Φ and Ψ of the lowest-energy representative of each cluster are reported in Table 1.

The 10 ns MC(JBW)/SD simulation of sialyl Lewis^x (Figure 4a) revealed that just the low-energy clusters A and B are populated, and the area of highest probability in torsional space

0947-6539/97/0310-1572 $ 17.50+.50/0 Chem. Eur. J. 1997, 3, No. 10

corresponds to a core conformation of −20 to −50° and an acid orientation of 110 to 140°. Clusters C and D are not populated. This result is in accord with the experimentally determined solution structure with respect to the core conformation of Lewis^x.[5] In addition, the conformational preferences of the neuraminic acid/galactose linkage are consistent with recent molecular modeling (MM2, continuum solvent model) and NMR studies (determination of $^3J_{CH}$ coupling constants across glycosidic linkages) by Tvaroska and Bizik.[6]

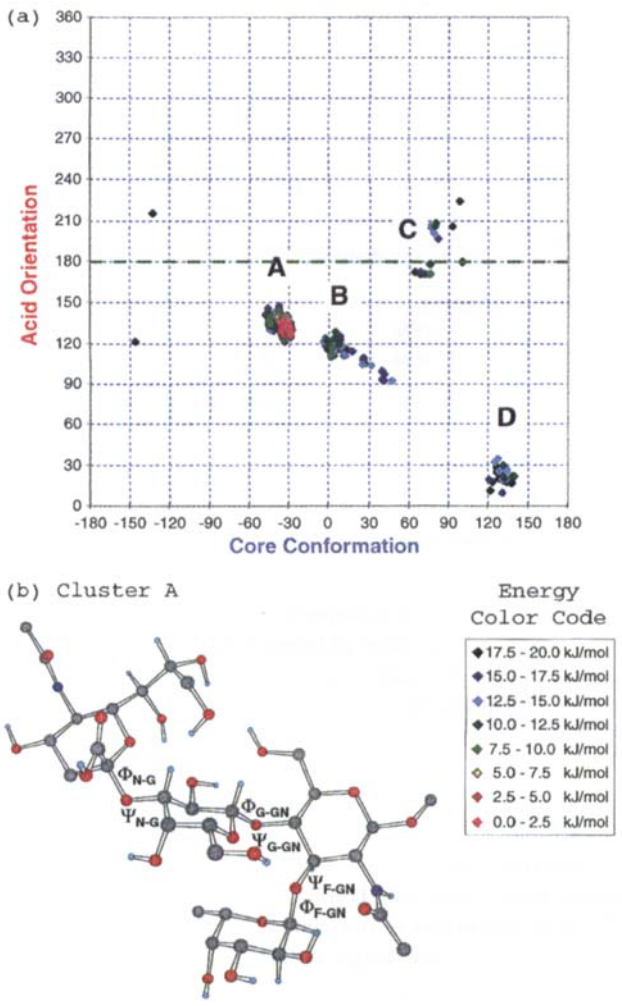

Figure 3. a) Internal coordinate plot from the SUMM [8] analysis of sialyl Lewis^x. b) Global minimum conformation of cluster A.

Table 1. Torsion angles (°) of interglycosidic linkages [a].

	Sia–Gal linkage		Gal–GlcNAc linkage		Fuc–GlcNAc linkage	
	Φ_{N-G}	Ψ_{N-G}	Φ_{G-GN}	Ψ_{G-GN}	Φ_{F-GN}	Ψ_{F-GN}
Cluster **A**	−69.9	9.5	49.2	6.7	47.6	19.0
Cluster **B**	−69.8	9.6	49.2	2.8	68.6	40.8
Cluster **C**	−70.7	7.2	22.5	170.2	32.5	176.0
Cluster **D**	−69.8	8.0	45.9	15.5	38.9	178.6

[a] Φ_{N-G}: Sia(C1)-Sia(C2)-Gal(O3)-Gal(C3); Ψ_{N-G}: Sia(C2)-Gal(O3)-Gal(C3)-Gal(H3); Φ_{G-GN}: Gal(H1)-Gal(C1)-GlcNAc(O4)-GlcNAc(C4); Ψ_{G-GN}: Gal(C1)-GlcNAc(O4)-GlcNAc(C4)-GlcNAc(H4); Φ_{F-GN}: Fuc(H1)-Fuc(C1)-GlcNAc(O3)-GlcNAc(C3); Ψ_{F-GN}: Fuc(C1)-GlcNAc(O3)-GlcNAc(C3)-GlcNAc(H3).

The computational technique was validated by calculating time-averaged $^3J_{CH}$ coupling constants across the glycosidic linkages using the structural information of the 10 ns MC(JBW)/SD simulation of sialyl Lewis^x in conjunction with the Karplus-type relationship developed by Tvaroska et al.[15] A remarkable match between experiment[5a, 6] and calculation was obtained: the deviation was always less than 0.5 Hz and in most instances even better (Table 2). This result suggests the chosen modeling technique to be highly suitable for simulating the conformational freedom of carbohydrates in solution.

Table 2. Calculated and observed [5a,6] $^3J_{CH}$ coupling constants.

	Obs. $^3J^{\pm}_{CH}$ (Hz)	Calcd $^3J_{CH}$ (Hz)	Time-averaged angle (°)
Sia(C2)–Gal(H3)	5.4	5.3	3.6
Gal(H1)–GlcNAc(C4)	2.8	2.4	50.6
Gal(C1)–GlcNAc(H4)	4.8	5.3	8.6
Fuc(H1)–GlcNAc(C3)	2.8	2.7	47.8
Fuc(C1)–GlcNAc(H3)	5.0–5.2	4.5	24.9

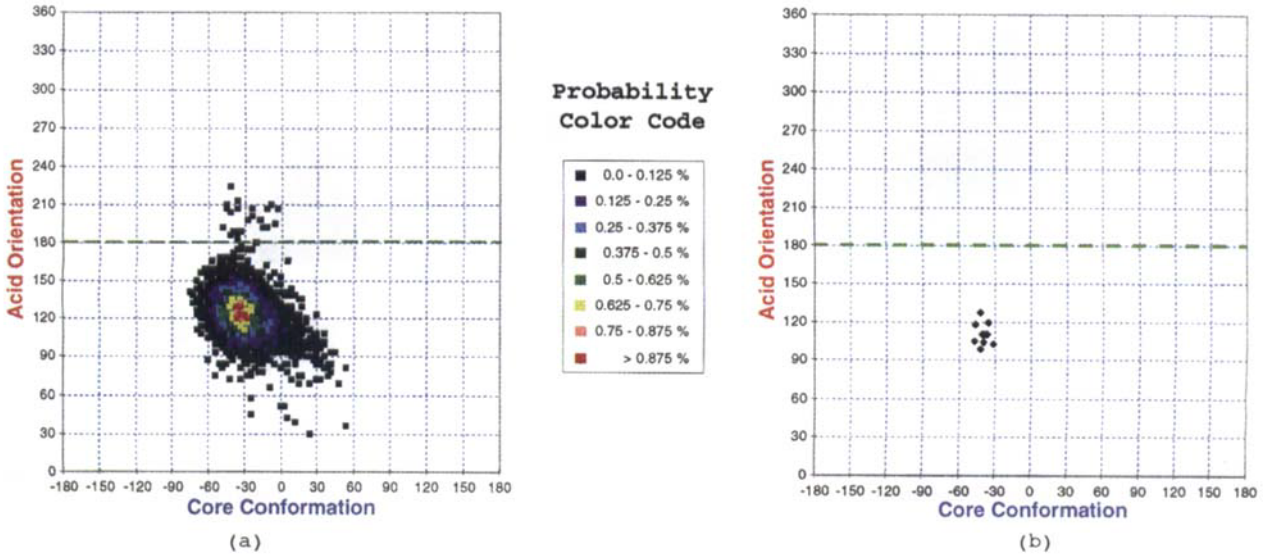

Figure 4. The bioactive conformation of sialyl Lewis^x. a) Analysis of the 10 ns MC(JBW)/SD simulation. b) Transfer NOE results [4].

  0947-6539/97/0310-1573 $ 17.50+.50/0

The method was further evaluated by comparing the calculated conformational freedom of sialyl Lewis^x with data derived from transfer-NOE experiments.[4] Interestingly, the bioactive area in the internal coordinate system (Figure 4b), determined by transfer-NOE NMR,[4] closely matches the region of highest probability (Figure 4a). The following model for the assessment of a compound's preorganization for binding to E-selectin can be derived at this point; it is based on the MC(JBW)/SD computational technique in conjunction with our probability analysis: A glycomimetic with a high probability of being in the bioactive area of torsional space has a good chance of being active, since it is preorganized for binding. Conversely, a compound which populates the bioactive region only partially or not at all has a low probability of being active.

Application of the model for assessing the preorganization of sialyl Lewis^x mimics—design of alternatives to neuraminic acid: Initially, α-hydroxy acid derivatives were considered as alternatives to neuraminic acid, since the spatial orientation of their carboxylic acid group may be controled by an appropriate choice of the configuration at Cα. To address this question, the lactic acid isomers **1** and **2** were analyzed as representatives of the (*R*) and (*S*) series of α-hydroxy acid derivatives (Figure 5). The MC(JBW)/SD data indicate that the (*R*) isomer **1** does not populate the bioactive area at all (Figure 5a), mainly owing to an unfavorable acid orientation. Thus, the (*R*) series would be expected to have a low affinity for E-selectin or even to be inactive. In contrast, the analysis of the (*S*) series (Figure 5b), represented by the (*S*)-lactic acid ether **2**, shows that both the core conformation *and* the acid orientation are inside the bioactive window, and one would therefore expect this series to be active.

In order to test these predictions, representatives of both series were synthesized (Scheme 1). The formation of the lactic acid ether bond, starting from the partially protected trisaccharide **3**,[16] was best performed by OH activation with di-*n*-butyltin oxide,[17] followed by treatment with the triflates **4** and **5**, respectively. The latter were obtained from the corresponding α-hydroxy carboxylic acids according to Degerbeck et al.[18] Removal of the protecting groups by hydrogenolysis finally provided the target compounds.

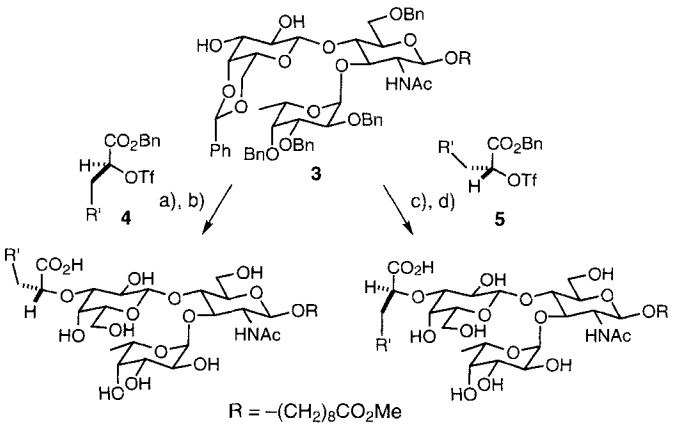

	R-Series	*S*-Series
R' = H:	**1**: IC_{50} > 10 mM	**2**: IC_{50} = 4.0 mM
R' = Ph:	**6**: IC_{50} > 10 mM	**7**: IC_{50} = 2.6 mM

Scheme 1. a) Bu_2SnO, MeOH, reflux; evaporated, then benzyl (*S*)-1-trifluoromethanesulfonyloxypropionate (**4**, R' = H) or benzyl (*S*)-2-phenyl-1-trifluoromethanesulfonyloxypropionate (**4**, R' = Ph), CsF, DME (100 and 63%, respectively); b) H_2, Pd/C, MeOH (60–65%); c) Bu_2SnO, MeOH, reflux; then benzyl (*R*)-1-trifluoromethanesulfonyloxypropionate (**5**, R' = H) or benzyl (*R*)-2-phenyl-1-trifluoromethanesulfonyloxypropionate (**5**, R' = Ph), CsF, DME (34%, 45% recovered starting material); d) H_2, 20% $Pd(OH)_2$/C, MeOH (70%).

As predicted, the (*R*) series of α-hydroxy acid derivatives was inactive in the E-selectin ligand binding assay.[19] In contrast, the (*S*) series of mimics was active, and the (*S*)-phenyllactic acid ether **7** even proved to be just 2–3 times less active than the lead structure, sialyl Lewis^x-$O(CH_2)_8CO_2Me$ (IC_{50} = 1.0 mM).

The predictive power of our computational tool was further tested by using it for the design of sialyl Lewis^x mimics in which

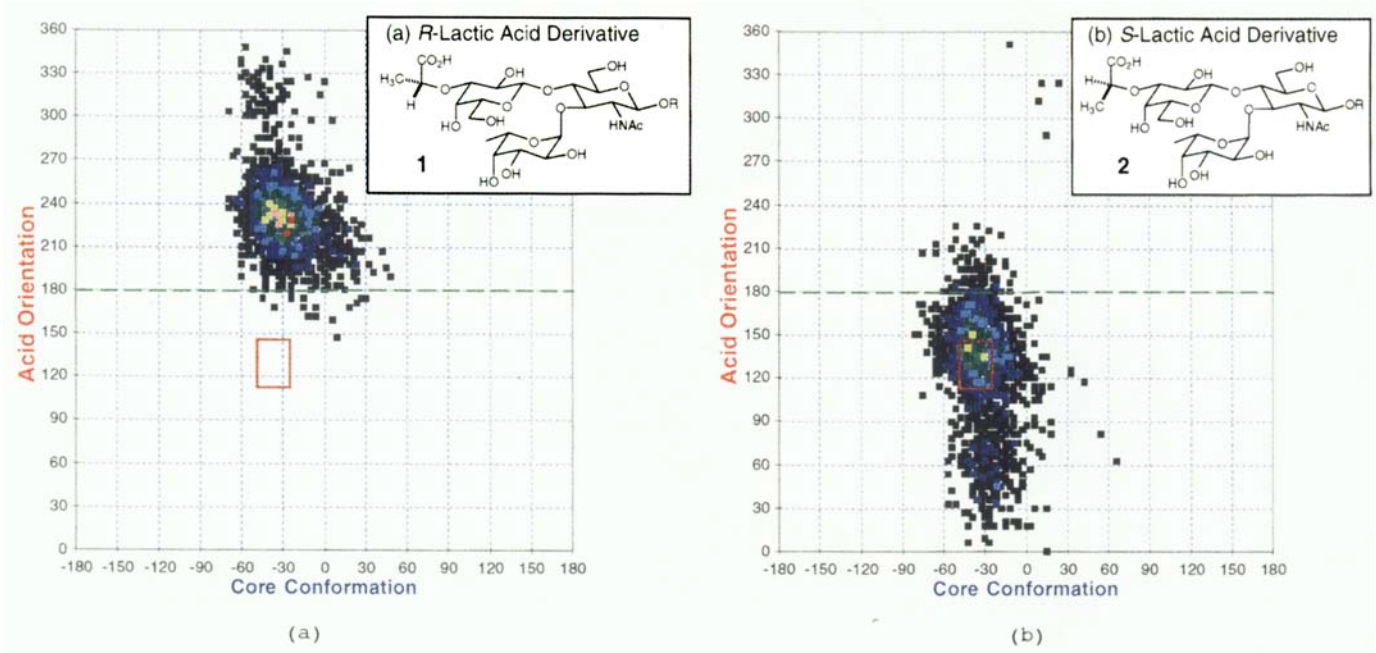

Figure 5. MC(JBW)/SD simulations of lactic acid derivatives.

0947-6539/97/0310-1574 $ 17.50+.50/0 *Chem. Eur. J.* **1997**, *3*, No. 10

both the neuraminic acid and the GlcNAc moieties had been replaced. As a replacement for GlcNAc, (*R*,*R*)-cyclohexanediol[20] was chosen, since this spacer should place the galactose and fucose units in a spatial arrangement similar to sialyl Lewis^x. The MC(JBW)/SD analyses were performed for the glycolic acid ether **8** as the structurally most simple analogue, as well as the diastereomeric (*R*)- and (*S*)-2-phenyllactic acid ethers **9** and **10** (Figure 6).

The MC(JBW)/SD conformational analysis of the glycolic acid ether **8** was performed for a total time of 2 ns. The transitions occurred once every 0.7 ps and the acceptance rate was 23%. The internal coordinate probability plot (Figure 6a) shows that the modifications do not affect the core conformation with respect to sialyl Lewis^x. This is supported by our observation of a very slightly enhanced bioactivity (ca. 65%) when the GlcNAc portion in sialyl Lewis^x is replaced by (*R*,*R*)-1,2-cyclohexanediol. The calculation (Figure 6a) suggests the acid/galactose linkage in the glycolic acid derivative **8** to be very flexible, and this mimic is therefore much less preorganized for binding than sialyl Lewis^x. In **8** the bioactive area at -20 to $-50°$ for the core conformation and 110 to 140° for the acid orientation is populated only to approximately 6% in contrast to 19% for sialyl Lewis^x. Consequently, the glycolic ether **8** should be less active than the lead structure or its (*R*,*R*)-1,2-cyclohexanediol analogue.

The MC(JBW)/SD simulations of the diastereomeric phenyllactic acid derivatives **9** and **10** (Figures 6b,c) were performed under identical conditions, and they again revealed the feasibility of replacing GlcNAc by (*R*,*R*)-cyclohexanediol. As before, the (*S*) series (Figure 6c) leads to compounds that have very similar conformational preferences to sialyl Lewis^x with respect to both core conformation and acid orientation. Since the (*S*)-phenyllactic acid ether **10** shows a population of the bioactive area of approximately 16%, it should be about as active as the lead structure, if one considers the preorganization as being the main factor influencing bioactivity. In contrast, compounds from the (*R*) series (Figure 6b) do not populate the bioactive area at all, and they should display a very low affinity to E-selectin.

Representative compounds of each series were synthesized (Scheme 2) and biologically evaluated in order to test our predictions. The 4,6-benzylidene acetal protected intermediate **12** was prepared in good yield by the acid-catalyzed reaction of the known tetrol **11**[21] with benzaldehyde dimethyl acetal. Activation of the remaining two OH groups with Bu_2SnO and treatment with an excess of benzyl (*R*)-2-phenyl-1-trifluoromethanesulfonyloxypropionate[18] resulted in selective etherification of the Gal-3-OH group. Hydrogenolysis finally gave the target molecule **10** in good overall yield.

The other target compounds **8**, **9**, **13**, and **14** shown in Figure 7 were prepared analogously. Their biological evaluation in the ligand-binding assay[19] supported the predicted trends from our conformational analysis. Thus, the glycolic acid ether **8** was less active than sialyl Lewis^x owing to its higher flexibility.

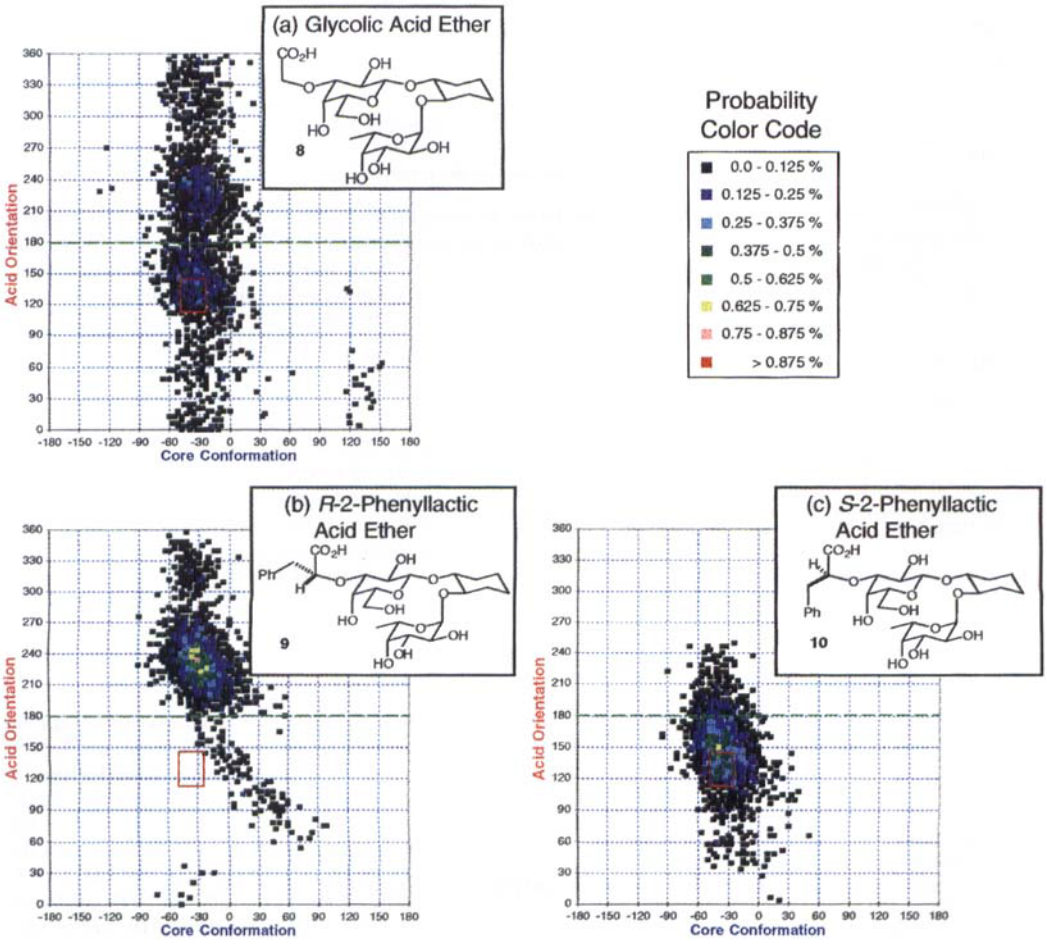

Figure 6. MC(JBW)/SD simulations of cyclohexanediol derivatives.

  0947-6539/97/0310-1575 $ 17.50+.50/0

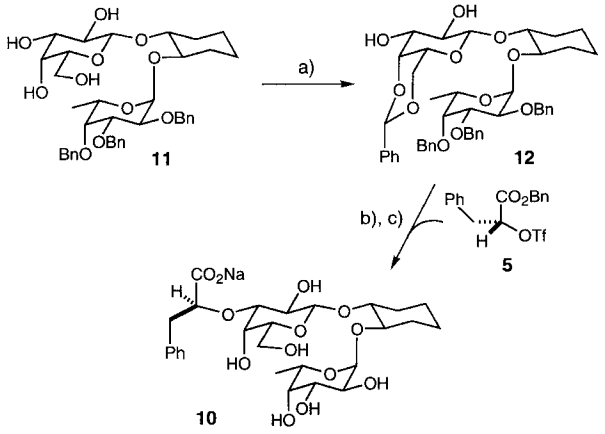

Scheme 2. Synthetic strategy for the target molecules. a) 3.0 equiv $PhCH(OMe)_2$, 0.5 equiv camphorsulfonic acid, MeCN, 35 °C, 0.75 h (87%); b) 1.5 equiv Bu_2SnO, MeOH, reflux, 2 h; evaporated; 5 equiv anhydrous CsF, 5 equiv benzyl (*R*)-2-phenyl-1-trifluoromethanesulfonyloxypropionate (**5**), 1,2-dimethoxyethane, RT, 2 h (70%); c) 20% $Pd(OH)_2/C$, H_2, dioxane/H_2O/HOAc, RT, 1 bar, 7 h, Dowex 50 (Na^+) (78%).

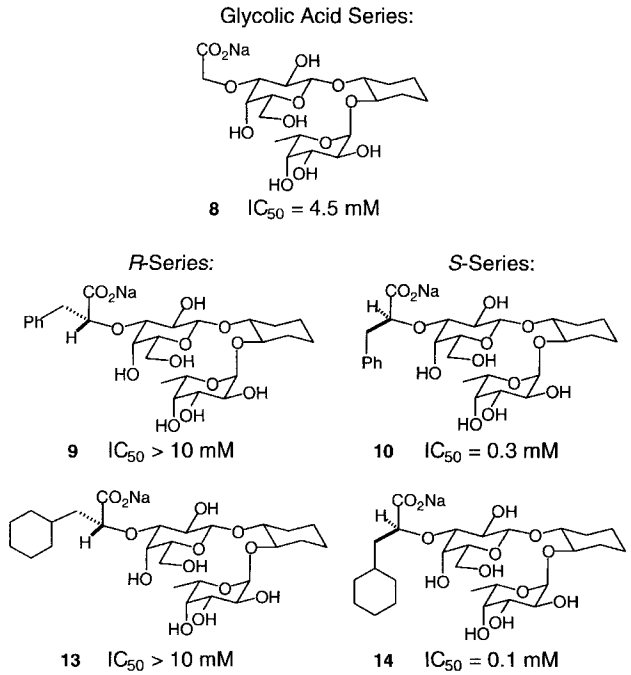

Figure 7. E-selectin binding results [20] (sialyl Lewis^x-$O(CH_2)_8CO_2Me$: IC_{50} = 1.0 mM).

Table 3. Modified Amber* force field paramaters (MacroModel Amber* format).

```
C          Stretching Interactions (STR)                Opt. Descriptor
C          -----------------------------                ---------------
C                      Bond Length   Constant Bond Moment Atm1 Atm2
1  O3 - H2                  0.9600   553.0000    -1.7631  C200 0000          M 1
1  O3 - H2                  0.9600   553.0000    -1.7631  C200 0000          M 1
C
C        Torsional Interaction (TOR)                    Opt. Descriptor
C        ---------------------------                    ---------------
C                          V1/2        V2/2       V3/2    Atm1 Atm2 Atm3 Atm4
C                            (Constants in Kcal/mol)
-2
4  O2 = C2 - CT - O3      -0.2600      0.5800     0.0000  0000 O300 0000 0000   A 2
4  O2 = C2 - CT - H1      -0.0200     -0.0170    -0.0035  0000 O300 0000 0000   A 1
4  O2 = C2 - CT - CT      -0.2100      0.1820    -0.0412  0000 O300 0000 0000   A 1
4  O3 - C2 - CT - O3       0.2600      0.5800     0.0000  0000 O200 0000 0000   M 1
4  O3 - C2 - CT - CT       0.2100      0.1820     0.0410  0000 O200 0000 0000   A 1
4  C2 - CT - O3 - 00       0.5930     -1.0200     0.6770  O2O3 0000 0000 0000   A 1
```

The (*R*)-α-hydroxy acid ether derivatives **9** and **13** were entirely inactive, since they do not populate the bioactive area. In contrast, compounds **10** and **14** from the (*S*)-α-hydroxy acid series were up to ten times more active than sialyl Lewis^x.

Summary

We have developed a computational tool for assessing the preorganization of sialyl Lewis^x mimics for binding to E-selectin. The model has been experimentally validated, and it allows a qualitative prediction of activity trends without requiring a detailed insight into the exact nature of the carbohydrate/lectin interaction. The agreement between predicted and observed activity trends suggests that the free binding energy is largely influenced by the preorganization of a compound and consequently by the entropy. The computational tool provides guidance for the design of new E-selectin ligands, since only candidate molecules that populate the bioactive area are considered to have a chance of being active. We are currently investigating the use of the calculated preorganization as a descriptor for quantitative structure–activity models.

Experimental Section

The force field: Amber* force field parameters[10] for α-alkoxy carboxylic acids were improved by first fitting partial atomic charges to electrostatic potential derived charges from high-level ab initio calculations and then adjusting the torsional parameters to reproduce the ab initio torsional drives for propionic acid (MP2/6-311G**//HF/6-311G**) and methoxyacetic acid. In the latter case two separate torsional drives about the $(HO_2C)-C\alpha$ bond and the $C\alpha-O$Me bond were performed at the MP2/6-31G**//HF/6-31G* level. The ab initio calculations were performed using GAMESS.[12] The new set of force constants is shown in Table 3.

Spectroscopic data of the target molecules.

(2*R*) 2-*O*-{1-*O*-[2-Acetamido-2-deoxy-4-*O*-(α-L-fucopyranosyl)-1-*O*-(1-methoxycarbonylnon-9-yl)-β-D-glucopyranosyl]-β-D-galactopyranos-3-yl}propanoic acid (1): ^{1}H NMR (500 MHz, D_2O): δ = 5.05 (d, J = 4.0 Hz, 1H), 4.78 (m, 1H), 4.46 (d, J = 8.2 Hz, 1H), 4.41 (d, J = 7.8 Hz, 1H), 4.05 (q, J = 6.9 Hz, 1H), 3.99 (d, J = 3.3 Hz, 1H), 3.95 (dd, J = 2.1, 11.8 Hz, 1H), 3.90–3.75 (m, 6H), 3.73 (d, J = 3.5 Hz, 1H), 3.71–3.59 (m, 3H), 3.62 (s, 3H), 3.56–3.47 (m, 4H), 3.38 (dd, J = 3.4, 10.0 Hz, 1H), 2.33 (t, J = 7.3 Hz, 2H), 1.96 (s, 3H), 1.58–1.43 (m, 4H), 1.32 (d, J = 7.0 Hz, 3H), 1.23 (s, 8H), 1.12 (d, J = 6.6 Hz, 3H); ^{13}C NMR (76 MHz, APT, D_2O): δ = 183.6 (C_q), 179.7 (C_q), 175.9 (C_q), 103.8 (CH), 102.7 (CH), 100.3 (CH), 82.1 (CH), 77.2 (CH), 77.1 (CH), 76.7 (CH), 76.6 (CH), 75.1 (CH), 73.7 (CH), 72.4 (CH_2), 71.4 (CH), 70.9 (CH), 69.5 (CH), 68.4 (CH), 67.2 (CH), 63.3 (CH_2), 61.4 (CH_2), 57.6 (CH), 53.8 (CH_3), 35.4 (CH_2), 30.3 (CH_2), 30.1 (CH_2), 29.9 (CH_2), 26.7 (CH_2), 26.0 (CH_2), 24.0 (CH_3), 20.6 (CH_3), 17.0 (CH_3); MS (FAB, THG): m/z = 794 [M^+ + Na]; $[\alpha]_D^{23} = -33.5$ (c = 0.6, H_2O).

(2*S*) 2-*O*-{1-*O*-[2-Acetamido-2-deoxy-4-*O*-(α-L-fucopyranosyl)-1-*O*-(1-methoxycarbonyl-non-9-yl)-β-D-glucopyranosyl]-β-D-galactopyranos-3-yl}propanoic acid (2): ^{1}H NMR (500 MHz, D_2O): δ = 5.06 (d, J = 3.8 Hz, 1H), 4.79 (q, J = 6.5 Hz, 1H), 4.48 (d, J = 8.1 Hz, 1H), 4.44 (d, J = 7.8 Hz, 1H), 4.02 (q, J = 6.9 Hz, 1H), 3.95 (dd, J = 1.5, 12.0 Hz, 1H), 3.93–3.78 (m, 7H), 3.76 (d, J = 3.0 Hz, 1H), 3.73–3.62 (m, 3H), 3.65 (s, 3H),

0947-6539/97/0310-1576 $ 17.50+.50/0 *Chem. Eur. J.* **1997**, *3*, No. 10

3.59–3.50 (m, 4H), 3.45 (dd, J = 3.1, 9.9 Hz, 1H), 2.35 (t, J = 7.4 Hz, 2H), 1.98 (s, 3H), 1.60–1.45 (m, 4H), 1.34 (d, J = 6.7 Hz, 3H), 1.26 (s, 8H), 1.14 (d, J = 6.5 Hz, 3H); ^{13}C NMR (76 MHz, APT, D_2O): δ = 183.7 (C_q), 179.7 (C_q), 175.9 (C_q), 103.3 (CH), 102.7 (CH), 100.4 (CH), 82.9 (CH), 78.3 (CH), 77.0 (CH), 76.7 (CH), 76.3 (CH), 75.0 (CH), 73.6 (CH), 72.4 (CH_2), 71.8 (CH), 70.9 (CH), 69.4 (CH), 68.4 (CH), 67.7 (CH), 63.4 (CH_2), 61.5 (CH_2), 57.6 (CH), 53.8 (CH_3), 35.4 (CH_2), 30.3 (CH_2), 30.1 (CH_2), 29.9 (CH_2), 26.7 (CH_2), 26.0 (CH_2), 24.0 (CH_3), 20.3 (CH_3), 17.1 (CH_3); MS (FAB, THG): m/z = 794 [M^+ + Na].

(2*R*) 2-*O*-{1-*O*-[2-Acetamido-2-deoxy-4-*O*-(α-L-fucopyranosyl)-1-*O*-(1-methoxycarbonylnon-9-yl)-β-D-glucopyranosyl]-β-D-galactopyranos-3-yl}-3-phenylpropanoic acid (6): ^{1}H NMR (500 MHz, D_2O): δ = 7.43–7.36 (m, 4H), 7.34–7.29 (m, 1H), 5.08 (d, J = 3.7 Hz, 1H), 4.79 (m, 1H), 4.50 (d, J = 8.2 Hz, 1H), 4.41 (d, J = 7.9 Hz, 1H), 4.19 (dd, J = 3.9, 10.0 Hz, 1H), 3.98 (dd, J = 2.4, 11.7 Hz, 1H), 3.92–3.80 (m, 6H), 3.72–3.64 (m, 2H), 3.68 (s, 3H), 3.62–3.46 (m, 6H), 3.42 (dd, J = 3.4, 8.5 Hz, 1H), 3.35 (dd, J = 3.3, 10.0 Hz, 1H), 3.21 (dd, J = 3.6, 14.1 Hz, 1H), 2.86 (dd, J = 10.0, 14.1 Hz, 1H), 2.38 (t, J = 7.4 Hz, 2H), 2.01 (s, 3H), 1.64–1.48 (m, 4H), 1.29 (s, 8H), 1.14 (d, J = 6.6 Hz, 3H); ^{13}C NMR (76 MHz, APT, D_2O): δ = 181.7 (C_q), 175.9 (C_q), 140.5 (C_q), 130.9 (CH), 130.5 (CH), 128.6 (CH), 103.5 (CH), 102.7 (CH), 100.3 (CH), 83.3 (CH), 83.0 (CH), 77.0 (CH), 76.6 (CH), 76.4 (CH), 75.0 (CH), 73.6 (CH), 72.4 (CH_2), 71.5 (CH), 70.9 (CH), 69.4 (CH), 68.3 (CH), 67.5 (CH), 63.1 (CH_2), 61.3 (CH_2), 57.6 (CH), 53.8 (CH_3), 35.5 (CH_2), 30.3 (CH_2), 30.0 (CH_2), 29.9 (CH_2), 26.7 (CH_2), 26.0 (CH_2), 24.0 (CH_3), 17.0 (CH_3); MS (FAB, THG): m/z = 870 [M^+ + Na], 848 [M^+ + H], 660 [M^+ − O(CH_2)$_8$$CO_2$Me].

(2*S*) 2-*O*-{1-*O*-[2-Acetamido-2-deoxy-4-*O*-(α-L-fucopyranosyl)-1-*O*-(1-methoxycarbonylnon-9-yl)-β-D-glucopyranosyl]-β-D-galactopyranos-3-yl}-3-phenylpropanoic acid (7): ^{1}H NMR (500 MHz, D_2O): δ = 7.38–7.30 (m, 4H), 7.29–7.23 (m, 1H), 5.05 (d, J = 3.8 Hz, 1H), 4.75 (m, 1H), 4.47 (d, J = 8.3 Hz, 1H), 4.34 (d, J = 7.8 Hz, 1H), 4.11 (dd, J = 4.7, 8.4 Hz, 1H), 3.93–3.71 (m, 9H), 3.70–3.59 (m, 3H), 3.64 (s, 3H), 3.57–3.42 (m, 4H), 3.28 (dd, J = 3.1, 9.8 Hz, 1H), 3.08 (dd, J = 4.7, 13.8 Hz, 1H), 2.93 (dd, J = 8.5, 13.8 Hz, 1H), 2.35 (t, J = 7.2 Hz, 2H), 1.97 (s, 3H), 1.60–1.43 (m, 4H), 1.25 (s, 8H), 1.12 (d, J = 6.6 Hz, 3H); ^{13}C NMR (76 MHz, APT, D_2O): δ = 181.5 (C_q), 178.9 (C_q), 175.1 (C_q), 139.1 (C_q), 130.5 (CH), 129.5 (CH), 127.6 (CH), 102.4 (CH), 101.9 (CH), 99.6 (CH), 83.2 (CH), 82.9 (CH), 76.2 (CH), 75.8 (CH), 75.3 (CH), 74.1 (CH), 72.8 (CH), 71.5 (CH_2), 71.2 (CH), 70.1 (CH), 68.6 (CH), 67.6 (CH), 66.9 (CH), 62.5 (CH_2), 60.6 (CH_2), 56.8 (CH), 53.0 (CH_3), 40.3 (CH_2), 34.6 (CH_2), 29.4 (CH_2), 29.2 (CH_2), 29.1 (CH_2), 25.9 (CH_2), 25.2 (CH_2), 23.2 (CH_3), 16.3 (CH_3); MS (FAB, THG): m/z = 870 [M^+ + Na], 848 [M^+ + H].

Sodium 2-*O*-{1-*O*-[(1*R*,2*R*) 2-*O*-(α-L-fucopyranosyl)cyclohexyl]-β-D-galactopyranos-3-yl}ethanoate (8): ^{1}H NMR (500 MHz, D_2O): δ = 4.95 (d, J = 3.9 Hz, 1H), 4.61 (q, J = 6.6 Hz, 1H), 4.49 (d, J = 7.8 Hz, 1H), 4.04 (m, 3H), 3.89 (dd, J = 3.3, 10.2 Hz, 1H), 3.77 (d, J = 3.4 Hz, 1H), 3.78–3.67 (m, 4H), 3.57 (dd, J = 4.5, 7.5 Hz, 1H), 3.54 (dd, J = 7.5, 9.6 Hz, 1H), 3.53–3.47 (m, 1H), 3.42 (dd, J = 3.2, 9.5 Hz, 1H), 2.13–2.01 (m, 2H), 1.67 (brs, 2H), 1.31–1.14 (m, 4H), 1.16 (d, J = 6.6 Hz, 3H); ^{13}C NMR (62.9 MHz, D_2O): δ = 182.2, 103.4, 99.2, 86.0, 81.8, 80.8, 78.2, 75.7, 73.6, 73.3, 72.1, 71.6, 70.2, 69.0, 65.2, 33.3, 32.8, 26.8, 18.9; MS (FAB, THG): m/z = 505 [M^+ + Na].

Sodium (2*R*) 2-*O*-{1-*O*-[(1*R*,2*R*) 2-*O*-(α-L-fucopyranosyl)cyclohexyl]-β-D-galactopyranos-3-yl}-3-phenylpropanoate (9): ^{1}H NMR (400 MHz, D_2O): δ = 7.28–7.20 (m, 4H), 7.19–7.12 (m, 1H), 4.80 (d, J = 3.9 Hz, 1H), 4.45 (q, J = 6.8 Hz, 1H), 4.27 (d, J = 7.7 Hz, 1H), 4.03 (dd, J = 4.0, 9.9 Hz, 1H), 3.71 (dd, J = 3.4, 10.3 Hz, 1H), 3.62–3.51 (m, 3H), 3.45 (dd, J = 8.1, 11.7 Hz, 1H), 3.40–3.29 (m, 4H), 3.26 (dd, J = 3.8, 8.3 Hz, 1H), 3.16 (dd, J = 3.3, 9.7 Hz, 1H), 3.04 (dd, J = 4.0, 14.0 Hz, 1H), 2.70 (dd, J = 10.0, 14.0 Hz, 1H), 1.98–1.86 (m, 2H), 1.53 (brs, 2H), 1.18–0.98 (m, 4H), 1.01 (d, J = 6.6 Hz, 3H); ^{13}C NMR (100.6 MHz, D_2O): δ = 180.9, 139.6, 130.1, 129.6, 127.8, 100.6, 96.4, 82.6, 79.0, 78.0, 75.4, 73.0, 70.7, 70.5, 68.8, 67.3, 66.9, 62.3, 40.1, 30.7, 30.1, 24.1, 16.2; MS (FAB, THG): m/z = 595 [M^+ + Na].

Sodium (2*S*) 2-*O*-{1-*O*-[(1*R*,2*R*)-2-*O*-(α-L-fucopyranosyl)-cyclohexyl]-β-D-galactopyranos-3-yl}-3-phenylpropanoate (10): ^{1}H NMR (500 MHz, D_2O): δ = 7.38–7.30 (m, 4H), 7.29–7.23 (m, 1H), 4.92 (d, J = 4.0 Hz, 1H), 4.55 (q, J = 6.7 Hz, 1H), 4.35 (d, J = 7.8 Hz, 1H), 4.11 (dd, J = 4.8, 8.5 Hz, 1H), 3.86 (d, J = 3.6 Hz, 1H), 3.84 (dd, J = 3.3, 10.5 Hz, 1H), 3.74 (d, J = 3.5 Hz, 1H), 3.71 (dd, J = 3.9, 10.5 Hz, 1H), 3.69–3.62 (m, 3H), 3.50 (ddd, J = 1.0, 4.5, 7.1 Hz, 1H), 3.48–3.41 (m, 1H), 3.43 (dd, J = 8.0, 9.7 Hz, 1H), 3.24 (dd, J = 3.5, 9.7 Hz, 1H), 3.09 (dd, J = 4.6, 14.0 Hz, 1H), 2.92 (dd, J = 8.8, 14.0 Hz, 1H), 2.06–1.97 (m, 2H), 1.63 (brs, 2H), 1.24–1.14 (m, 4H), 1.13 (d, J = 7.0 Hz, 3H); ^{13}C NMR (100.6 MHz, APT, D_2O): δ = 139.5 (C_q), 130.7 (2 CH), 129.9 (2 CH), 128.0 (CH), 100.8 (CH), 96.8 (CH), 84.0 (CH), 83.3 (CH), 79.6 (CH), 78.4 (CH), 75.6 (CH), 73.3 (CH), 71.4 (CH), 70.9 (CH), 69.2 (CH), 67.7 (CH), 67.4 (CH), 62.8 (CH_2), 40.6 (CH_2), 30.9 (CH_2), 30.4 (CH_2), 24.4 (2 CH_2), 16.6 (CH_3); MS (FAB, THG): m/z = 595 [M^+ + Na], 573 [M^+ + H].

Sodium (2*R*) 3-cyclohexyl-2-*O*-{1-*O*-[(1*R*,2*R*) 2-*O*-(α-L-fucopyranosyl)cyclohexyl]-β-D-galactopyranos-3-yl}propanoate (13): ^{1}H NMR (400 MHz, D_2O): δ = 4.88 (d, J = 3.9 Hz, 1H), 4.54 (q, J = 6.7 Hz, 1H), 4.39 (d, J = 7.7 Hz, 1H), 3.96 (dd, J = 4.5, 8.8 Hz, 1H), 3.92 (d, J = 3.2 Hz, 1H), 3.83 (dd, J = 3.41, 10.4 Hz, 1H), 3.71–3.56 (m, 5H), 3.50–3.39 (m, 3H), 3.29 (dd, J = 3.3, 9.9 Hz, 1H), 2.06–1.93 (m, 2H), 1.71 (br d, J = 12.4 Hz, 1H), 1.65–1.31 (m, 9H), 1.25–0.98 (m, 7H), 1.10 (d, J = 6.6 Hz, 3H), 0.94–0.75 (m, 2H); MS (FAB, THG): m/z = 601 [M^+ + Na], 579 [M^+ + H]; $[\alpha]_D^{23}$ = − 42.4 (c = 0.4, H_2O).

Sodium (2*S*) 3-cyclohexyl-2-*O*-{1-*O*-[(1*R*,2*R*) 2-*O*-(α-L-fucopyranosyl)cyclohexyl]-β-D-galactopyranos-3-yl}propanoate (14): ^{1}H NMR (500 MHz, D_2O): δ = 4.93 (d, J = 3.8 Hz, 1H), 4.58 (q, J = 6.4 Hz, 1H), 4.43 (d, J = 7.5 Hz, 1H), 3.91 (dd, J = 3.5, 9.0 Hz, 1H), 3.88–3.83 (m, 2H), 3.75 (d, J = 3.3 Hz, 1H), 3.73–3.64 (m, 4H), 3.57–3.53 (m, 1H), 3.49 (dd, J = 7.3, 9.0 Hz, 1H), 3.50–3.43 (m, 1H), 3.33 (dd, J = 3.2, 9.2 Hz, 1H), 2.10–1.99 (m, 2H), 1.73 (br d, J = 12.0 Hz, 1H), 1.69–1.44 (m, 9H), 1.29–1.07 (m, 7H), 1.14 (d, J = 6.5 Hz, 3H), 0.96–0.80 (m, 2H); MS (FAB, THG): m/z = 601 [M^+ + Na].

Received: December 4, 1996 [F 543]
Revised version: April 4, 1997

[1] a) R. A. Dwek, *Chem. Rev.* **1996**, *96*, 683–720; b) W. I. Weis, K. Drickamer, *Annual Rev. Biochem.* **1996**, *65*, 441–473.

[2] a) S. R. Sharar, R. K. Winn, J. M. Harlan, *Springer Semin. Immunopathol.* **1995**, *16*, 359–378; b) F. Dasgupta, B. N. N. Rao, *Exp. Opin. Invest. Drugs* **1994**, *3*, 709–724; c) J. K. Welply, J. L. Keene, J. J. Schmuke, S. C. Howard, *Biochim. Biophys. Acta* **1994**, *1197*, 215–226; d) R. P. McEver, *Curr. Opin. Immunol.* **1994**, *6*, 75–84; e) S. D. Rosen, C. R. Bertozzi, *Curr. Opin. Cell Biol.* **1994**, *6*, 663–673; f) M. P. Bevilacqua, *Annu. Rev. Immunol.* **1993**, *11*, 767–804; g) T. A. Springer, *Cell* **1994**, *76*, 301–314; h) A. Varki, *Proc. Natl. Acad. Sci. USA* **1994**, *91*, 7390–7397; i) R. P. McEver, K. L. Moore, R. D. Cummings, *J. Biol. Chem.* **1995**, *270*, 11025–11028.

[3] a) H. Ohmoto, K. Nakamura, T. Inoue, N. Kondo, Y. Inoue, K. Yoshino, H. Kondo, H. Ishida, M. Kiso, A. Hasegawa, *J. Med. Chem.* **1996**, *39*, 1339–1343; b) A. Hasegawa, M. Kato, T. Ando, H. Ishida, M. Kiso, *Carbohydr. Res.* **1995**, *274*, 165–181; c) A. Hasegawa, T. Ando, M. Kato, H. Ishida, M. Kiso, *ibid.* **1994**, *257*, 67–80; d) M. Yoshida, A. Uchimura, M. Kiso, A. Hasegawa, *Glycoconjugate J.* **1993**, *10*, 3–15; e) A. Hasegawa, K. Fushimi, H. Ishida, M. Kiso, *J. Carbohydr. Chem.* **1993**, *12*, 1203–1216; f) B. K. Brandley, M. Kiso, S. Abbas, P. Nikrad, O. Srivasatava, C. Foxall, Y. Oda, A. Hasegawa, *Glycobiology* **1993**, *3*, 633–639; g) D. Tyrrell, P. James, N. Rao, C. Foxall, S. Abbas, F. Dasgupta, M. Nashed, A. Hasegawa, M. Kiso, D. Asa, J. Kidd, B. K. Brandley, *Proc. Natl. Acad. Sci. USA* **1991**, *88*, 10372–10376; h) W. Stahl, U. Sprengard, G. Kretzschmar, H. Kunz, *Angew. Chem.* **1994**, *106*, 2186–2188; *Angew. Chem. Int. Ed. Engl.* **1994**, *33*, 2096–2098; i) G. Thoma, F. Schwarzenbach, R. O. Duthaler, *J. Org. Chem.* **1996**, *61*, 514–524.

[4] a) R. M. Cooke, R. S. Hale, S. G. Lister, G. Shah, M. P. Weir, *Biochemistry* **1994**, *33*, 10591–10596; b) P. Hensley, P. J. McDevitt, I. Brooks, J. J. Trill, J. A. Feild, D. E. McNulty, J. R. Connor, D. E. Griswold, N. V. Kumar, K. D. Kopple, S. A. Carr, B. J. Dalton, K. Johanson, *J. Biol. Chem.* **1994**, *269*, 23949–23958; c) K. Scheffler, B. Ernst, A. Katopodis, J. L. Magnani, W. T. Wang, R. Weisemann, T. Peters, *Angew. Chem.* **1995**, *107*, 2034–2037; *Angew. Chem. Int. Ed. Engl.* **1995**, *34*, 1841–1844.

[5] a) T. J. Rutherford, D. G. Spackman, P. J. Simpson, S. W. Homans, *Glycobiology* **1994**, *4*, 59–68; b) C. Mukhopadhyay, K. E. Miller, C. A. Bush, *Biopolymers* **1994**, *34*, 21–29; c) Y. Ichikawa, Y.-C. Lin, D. P. Dumas, G.-J. Shen, E. Garcia-Junceda, M. A. Williams, R. Bayer, C. Ketcham, L. E. Walker, J. C. Paulson, C.-H. Wong, *J. Am. Chem. Soc.* **1992**, *114*, 9283–9298; d) H. C. Siebert, G. Reuter, R. Schauer, C. W. v. d. Lieth, J. Dabrowski, *Biochemistry* **1992**, *31*, 6962–6971; e) G. E. Ball, R. A. O'Neill, J. E. Schultz, J. B. Lowe, B. W. Weston, J. O. Nagy, E. G. Brown, C. J. Hobbs, M. D. Bednarsky, *J. Am. Chem. Soc.* **1992**, *114*, 5449–5451; f) J. Breg, L. M. J. Kroon-Batenburg, G. Strecker, J. Montreuil, J. F. G. Vliegenthart, *Eur. J. Biochem.* **1989**, *178*, 727–739; g) R. U. Lemieux, K. Bock, L. T. J. Delbaere, S. Koto, V. S. Rao, *Can. J. Chem.* **1980**, *58*, 631–653.

  0947-6539/97/0310-1577 $ 17.50+.50/0

[6] a) F. Bizik, I. Tvaroska, *Chem. Papers* **1996**, *50*, 84–96; for a detailed conformational analysis of the rigid Lewis^x core, see b) A. Imberty, E. Mikros, J. Koca, R. Mollicone, R. Oriol, S. Pérez, *Glycoconjugate J.* **1995**, *12*, 331–349.
[7] B. J. Graves, R. L. Crowther, C. Chandran, J. M. Rumberger, S. Li, K.-S. Huang, D. H. Presky, P. C. Familletti, B. A. Wolitzky, D. K. Burns, *Nature* **1994**, *367*, 532–538.
[8] J. M. Goodman, W. C. Still, *J. Comput. Chem.* **1991**, *12*, 1110–1117.
[9] H. Senderowitz, F. Guarnieri, W. C. Still, *J. Am. Chem. Soc.* **1995**, *117*, 8211–8219.
[10] F. Mohamadi, N. G. J. Richards, W. C. Guida, R. Liskamp, M. Lipton, C. Caufield, G. Chang, T. Hendrickson, W. C. Still, *J. Comput. Chem.* **1990**, *11*, 440–467. The asterisk in Amber* indicates that a modified Amber force field was used.
[11] a) H. Senderowitz, C. Parish, W. C. Still, *J. Am. Chem. Soc.* **1996**, *118*, 2078–2086; b) for further ab initio studies on carbohydrate model compounds, see: I. Tvaroska, J. P. Carver, *J. Phys. Chem.* **1994**, *98*, 9477–9485.
[12] M. W. Schmidt, K. K. Baldridge, J. A. Boatz, S. T. Elbert, M. S. Gordon, J. H. Jensen, S. Koseki, N. Matsunaga, K. A. Nguyen, S. J. Su, T. L. Windus, M. Dupuis, J. A. Montgomery, *J. Comput. Chem.* **1993**, *14*, 1347–1363.
[13] G. D. Rockwell, T. B. Grindley, *Aust. J. Chem.* **1996**, *49*, 379–390.
[14] W. C. Still, A. Tempczyk, R. C. Hawley, T. Hendrickson, *J. Am. Chem. Soc.* **1990**, *112*, 6127–6129.
[15] a) I. Tvaroska, M. Hricovini, E. Petrakova, *Carbohydrate Res.* **1989**, *189*, 359–362; b) I. Tvaroska, *ibid.* **1990**, *206*, 55–64.
[16] a) R. M. Ippolito, W. Haque, C. Jiang, R. Hanna, A. P. Venot, P. V. Nikrad, M. A. Kashem, R. H. Smith, WO 9222564 (**1992**), Alberta Research Council, Can.; b) O. Srivastava, R. Ippolito, G. Srivastava, R. Szweda, T. Ohuchi, WO 9616071 (**1996**), Glycomed, USA.
[17] a) M. A. Nashed, L. Anderson, *Tetrahedron Lett.* **1976**, *39*, 3503–3506; b) N. Nagashima, M. Ohno, *Chem. Lett.* **1987**, 141–144.
[18] F. Degerbeck, B. Fransson, L. Grehn, U. Ragnarsson, *J. Chem. Soc. Perkin Trans. 1* **1993**, 11–14.
[19] The binding assay was performed by Dr. J. Magnani (GlycoTech, Rockville, USA). Wells in a microtiter plate (plate 1, Falcon probind™) were coated with E-selectin/hIg chimera by incubation of 100 μL of the purified chimeric protein at a concentration of 200 ng/well in 50 mM Tris, 0.15 M NaCl, 2 mM $CaCl_2$, pH 7.4 (Tris–Ca^{2+}). After 2 h, 100 μL of a 1:1 mixture of 1% BSA in Tris–Ca^{2+} and Stabilcoat™ were added to each well and incubated at 22 °C to block nonspecific binding. During this incubation, inhibitory test compounds (diluted in Tris–Ca^{2+}, 1% BSA) were titrated by a twofold serial dilution in a second U-shaped bottom low-bind microtiter plate (plate 2, Costar). An equal volume of a preformed complex of a biotinylated sialyl Lewis^a polymer and horseradish peroxidase-labeled streptavidin (KPL, Gathersburg, MD) at 1 μg/mL in Tris–Ca^{2+}, 1% BSA was added to each well. After 2 h at 22 °C, plate 1 was washed with Tris–Ca^{2+}, and 100 μL/well was transferred from plate 2 to plate 1. The binding reaction was allowed to proceed for 2 h at 22 °C while rocking. Plate 1 was then washed with Tris–Ca^{2+} and 100 μL of TMB substrate reagent (KPL, Gathersburg, MD) was added to each well. After 3 min, the colorimetric reaction was stopped by adding 100 μL/well of 1 M H_3PO_4, and the optical density was determined at 450 nm.
[20] A. Toepfer, G. Kretzschmar, E. Bartnik, *Tetrahedron Lett.* **1995**, *36*, 9161–9164.
[21] A. Toepfer, G. Kretzschmar, E. Bartnik, D. Seifge, EP 671409 (**1995**), Hoechst A.-G., Germany.

  0947-6539/97/0310-1578 $ 17.50+.50/0